doi:10.1016/j.jmb.2007.12.079 J. Mol. Biol. (2008) 377, 565–574

JMB

Available online at www.sciencedirect.com

ScienceDirect

ELSEVIER

Mutations Enhance the Aggregation Propensity of the Alzheimer's Aβ Peptide

Woojin Kim and Michael H. Hecht*

Department of Chemistry, Princeton University, Princeton, NJ 08544, USA

Received 31 October 2007; received in revised form 22 December 2007; accepted 31 December 2007
Available online 11 January 2008

Aggregation of the amyloid β (Aβ) peptide plays a key role in the molecular etiology of Alzheimer's disease. Despite the importance of this process, the relationship between the sequence of Aβ and the propensity of the peptide to aggregate has not been fully elucidated. The sequence determinants of aggregation can be revealed by probing the ability of amino acid substitutions (mutations) to increase or decrease aggregation. Numerous mutations that decrease aggregation have been isolated by laboratory-based studies. In contrast, very few mutations that increase aggregation have been reported, and most of these were isolated from rare individuals with early-onset familial Alzheimer's disease. To augment the limited data set of clinically derived mutations, we developed an artificial genetic screen to isolate novel mutations that increase aggregation propensity. The screen relies on the expression of Aβ–green fluorescent protein fusion in *Escherichia coli*. In this fusion, the ability of the green fluorescent protein reporter to fold and fluoresce is inversely correlated with the aggregation propensity of the Aβ sequence. Implementation of this screen enabled the isolation of 20 mutant versions of Aβ with amino acid substitutions at 17 positions in the 42-residue sequence of Aβ. Biophysical studies of synthetic peptides corresponding to sequences isolated by the screen confirm the increased aggregation propensity and amyloidogenic behavior of the mutants. The mutations were isolated using an unbiased screen that makes no assumptions about the sequence determinants of aggregation. Nonetheless, all 16 of the most aggregating mutants contain substitutions that reduce charge and/or increase hydrophobicity. These findings provide compelling evidence supporting the hypothesis that sequence hydrophobicity is a major determinant of Aβ aggregation.

Keywords: amyloid beta; aggregation; Alzheimer's disease; amyloid fibril; high-throughput screen

Edited by K. Kuwajima

Introduction

Postmortem studies of the brains of patients with Alzheimer's disease (AD) reveal significant quantities of senile plaque. Biochemical analyses of amyloid fibrils in these plaques indicate that amyloid β (Aβ) peptides are the primary components of the fibrils.[1,2] These Aβ peptides are produced by proteolytic cleavage of the amyloid precursor protein (APP). Because cleavage of APP can occur at several sites, Aβ peptides occur in several different lengths, with the 40-residue Aβ40 and the 42-residue Aβ42 being the most abundant. Although Aβ40 is produced in larger amounts, Aβ42 aggregates more readily, and increased ratios

*Corresponding author. E-mail address: hecht@princeton.edu.

Present address: W. Kim, Division of Hematology–Oncology, Children's Hospital, Harvard Medical School, Boston, MA, USA.

Abbreviations used: Aβ, amyloid β; AD, Alzheimer's disease; APP, amyloid precursor protein; FAD, familial Alzheimer's disease; GFP, green fluorescent protein; WM, white mutant; ThT, thioflavin T; EM, electron microscopy; RP, reverse phase.

of Aβ42/Aβ40 have been observed in the brains of AD patients.[3,4]

The molecular details of Aβ aggregation and the mechanism through which this aggregation causes AD are not fully understood. Nonetheless, a large number of studies support the "amyloid cascade" hypothesis,[5] which posits that accumulation of aggregated Aβ initiates a multistep cascade that ultimately leads to AD. Several lines of evidence support this hypothesis. First, genetic studies show that several forms of familial Alzheimer's disease (FAD) are caused by mutations either in APP or in enzymes that process APP. Both classes of mutations increase the production and/or aggregation of Aβ42 and lead to the early onset of AD.[6–8] Second, early-onset AD is also observed in Down syndrome, wherein trisomy of chromosome 21, which encodes APP, leads to increased production of Aβ42.[9–12] Third, construction of transgenic animals, including nematodes, fruit flies, and mice, has demonstrated that introduction of APP and/or Aβ produces cognitive and behavioral impairments.[13–15] Finally, studies of enzymes that metabolize Aβ confirm the relationship between Aβ accumulation and AD. For example, decreased expression of insulin-degrading enzyme or neprilysin, both of which are known to degrade Aβ, leads to increased accumulation of Aβ and, ultimately, to AD. In contrast, overexpression of these enzymes reduces Aβ levels and attenuates Aβ-related memory deficit.[16–20] Together, these studies provide a compelling case for the role of Aβ aggregation in the pathogenesis of AD.

Although Aβ accumulation and aggregation clearly play a role in AD, recent studies indicate that the insoluble fibrils themselves may not be the toxic species. Instead, it now appears that oligomers or intermediates in the aggregation process are the major toxic species in AD. For example, Lesne *et al.* demonstrated that extracellular accumulation of a 56-kDa soluble oligomer of Aβ42 (presumably a dodecamer) causes memory deficits in transgenic mice.[21] Similarly, Walsh *et al.* demonstrated that small oligomers of Aβ inhibit long-term potentiation of neurons, resulting in memory deficits, whereas monomers or fibrils of Aβ show no effect.[22,23]

To enhance understanding of the molecular etiology of AD, we and others have probed the amino acid sequence determinants of Aβ aggregation.[24–29] Previously, our laboratory developed an artificial genetic system to screen for mutations in the sequence of Aβ42 that prevent aggregation.[24] By using this system to screen randomly generated libraries of mutations, we demonstrated that replacement of nonpolar residues with polar residues inhibited aggregation and caused dramatic increases in the solubility of Aβ42. More recently, we also showed that at many positions in the Aβ42 sequence, random mutations of nonpolar residues to other nonpolar residues had little or no effect, thereby demonstrating that "generic" hydrophobic residues—rather than particular nonpolar side chains—are sufficient to promote the aggregation of Aβ42.

Complementary studies by both Williams *et al.* and Morimoto *et al.* used proline-scanning mutagenesis to demonstrate that disruption of the β-sheet regions of Aβ decreases aggregation propensity.[27,28] Thus, mutagenesis experiments have shown that both sequence hydrophobicity and β-sheet propensity are key determinants of aggregation. Experimental and bioinformatics approaches by Chiti *et al.* support these findings, both for Aβ42 and for other amyloidogenic proteins.[29]

In addition to the laboratory-generated mutations described above, naturally occurring mutants in the human population provide insights into the sequence determinants of Aβ aggregation. Several examples of familial early-onset AD are caused by mutations in Aβ that increase its aggregation propensity. For example, the Dutch mutant, Glu22→Gln, increases Aβ aggregation and leads to early-onset AD.[30]

Laboratory-based studies of the sequence determinants of Aβ aggregation have focused primarily on mutations that *decrease* aggregation. In contrast, genetic studies of early-onset FAD in the human population have discovered mutations that *increase* aggregation propensity. In this latter class, however, only a few mutants are known, presumably because those mutations that cause the most dramatic increase in aggregation are lethal and do not survive in the population. To augment the clinically isolated collection of aggregation-prone mutants in Aβ, we have developed an unbiased screen for mutations that increase aggregation. Here we describe the implementation of this screen to isolate a collection of mutations that increase aggregation propensity beyond that of wild-type Aβ.

Results

Amino acid substitutions produce variants of Aβ with increased propensities to aggregate

Previously, our laboratory described a high-throughput screen for mutations in Aβ42 that inhibit aggregation. Our screen relied on the fusion of Aβ42 to green fluorescent protein (GFP). In such fusions, the correct folding and fluorescence of GFP depend on the solubility of Aβ42.[24,31] Consequently, fusions of wild-type Aβ42 to GFP yield colorless samples. However, mutations in Aβ42 that inhibit aggregation allow GFP to fold and yield fluorescent samples. This fusion system was adapted to high throughput screening screen expressing the fusion protein in *Escherichia coli* and screening for green colonies on Petri dishes. We have used this system previously (i) to develop an unbiased screen for random mutations that diminish Aβ42 aggregation;[24] (ii) to probe the importance of side chains at positions 41 and 42 in causing Aβ42 to aggregate more readily than Aβ40;[26] (iii) to demonstrate that generic hydrophobic residues (compared to specific side chains) at many positions in the Aβ42 sequence are sufficient to

promote aggregation and fibrilogenesis;[25] and (iv) to develop a high-throughput screen for small-molecule inhibitors of Aβ42 aggregation.[32]

In the current report, we demonstrate that Aβ–GFP fusions can be used not only to isolate *inhibitors of aggregation* (either mutations in the sequence or exogenous small molecules) but also to find amino acid substitutions that actually *enhance* aggregation propensity.

Isolating mutants with enhanced aggregation propensity required that we use the Aβ–GFP screen in an inverse form: Instead of searching for rare green colonies (indicating Aβ solubility and GFP folding) amidst collections of white colonies, we sought to isolate rare white colonies (indicating Aβ aggregation and GFP misfolding) amidst collections of green samples. This inverse screen was made possible by modifying our original screen in two significant ways: First, instead of using fusions to Aβ42, we used fusions to the less aggregating Aβ40. Second, instead of running the screen at 37 °C, we ran it at 30 °C, where aggregation occurs more slowly. With these modifications, wild-type Aβ40–GFP fusions produce colonies that are slightly fluorescent.[26] Thus, we could isolate mutants that enhance aggregation by searching for rare white colonies amidst collections of slightly green colonies.

We constructed a library of random mutations in Aβ40 using error-prone PCR. GFP fusions to this library were expressed at 30 °C and screened for white colonies, indicating enhanced aggregation relative to the wild-type Aβ40–GFP fusion. In principle, however, white colonies could result either from amino acid substitutions in Aβ40 that increase its aggregation propensity or from spurious mutations, including (i) deletion of all or part of the GFP construct; (ii) frameshifts and/or stop codons; and (iii) diminished protein expression. To ensure that the white phenotype was *not* due to deletions, frameshifts, stop codons, or reduced expression, all white colonies were assayed for protein expression by SDS-PAGE (data not shown), and only those clones that expressed at levels similar to those of the wild-type Aβ40–GFP fusion were pursued for further studies. The sequences of these mutants are shown in Fig. 1.

The aggregation propensities of the mutant sequences of Aβ40 were compared to those of wild-type Aβ40 (and Aβ42) by measuring the fluorescence of cultures expressing the corresponding GFP fusions. As shown in previous work, there is a direct correlation between the fluorescence of such cultures and the solubility of the Aβ–GFP fusion: Fusions yielding lower fluorescence are less soluble.[24–26] Figure 2 shows that mutant versions of Aβ40–GFP fusions display a range of fluorescence. Some are similar to wild-type Aβ40–GFP fusions, while others are considerably lower. Strikingly, some of the mutations in Aβ40 produce signals even lower than those of wild-type Aβ42, indicating that these amino acid replacements cause Aβ40 to aggregate even more readily than wild-type Aβ42. For example, GFP fusions to WM1–WM5 (WM: white mutant) show less fluorescence than the wild-type Aβ42–GFP fusion. Considering that WM1–WM5 are mutants of Aβ40 and that wild-type Aβ40 is much less prone to aggregate than wild-type Aβ42,[3,4,33] these results indicate that the amino acid substitutions present in WM1–WM5 exert a substantial effect on the aggregation propensity of Aβ.

Mutant peptides have high propensities to form amyloid

To confirm that mutations isolated by screening GFP fusions in *E. coli* actually increase the aggregation propensity of the Aβ peptide in isolation, we compared the rates of aggregation of mutant and

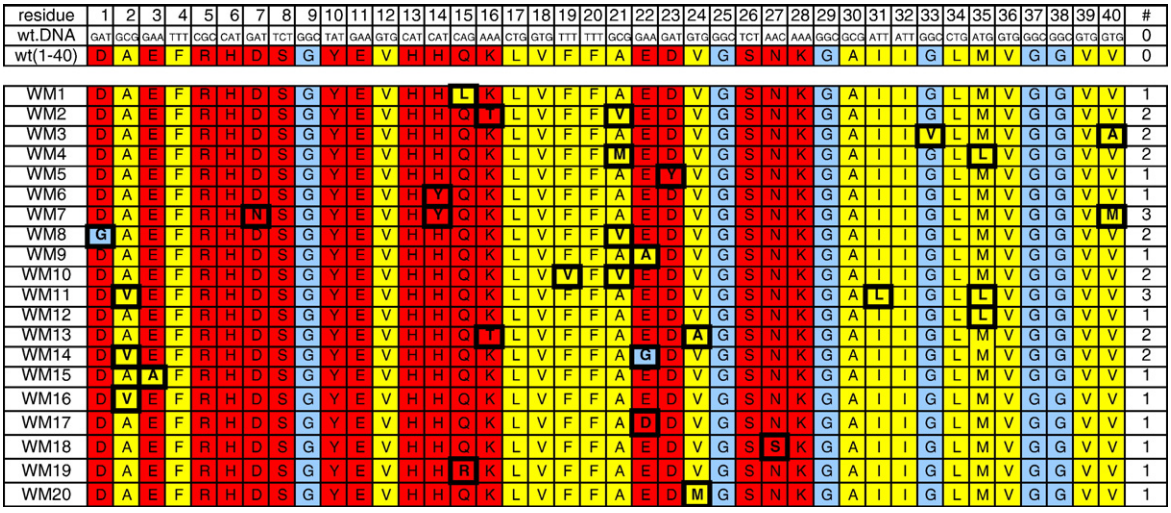

Fig. 1. Amino acid substitutions that enhance the aggregation propensity of Aβ. Mutants of Aβ40 with enhanced aggregation propensities are listed in order of decreasing aggregation propensity. WM, white mutant. Red, yellow, and blue designate polar, nonpolar, and glycine, respectively. The number of amino acid substitutions is listed at the right of each sequence.

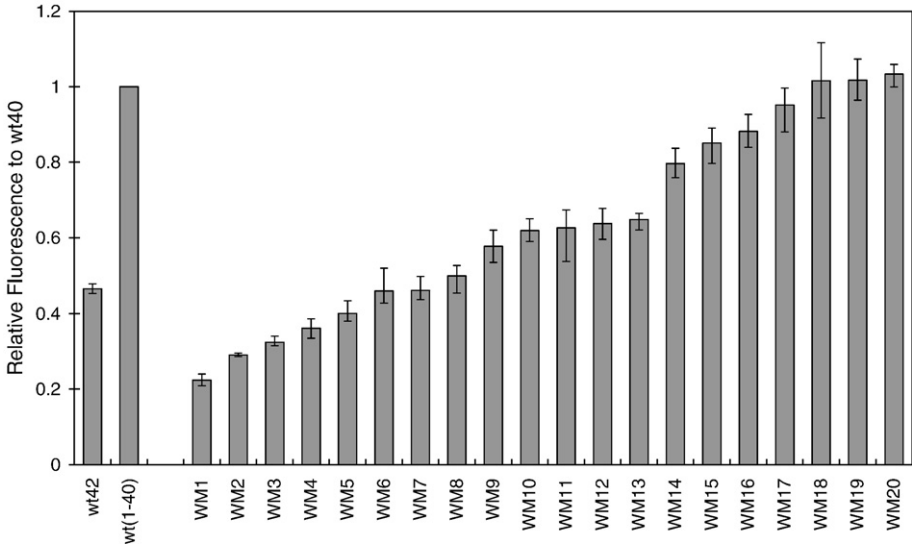

Fig. 2. Fluorescence of cultures expressing fusions of mutant forms of Aβ40 to GFP. Values are plotted relative to the wild-type Aβ40–GFP fusion. Low values indicate that aggregation of the Aβ fusion partner causes GFP to misfold, thereby preventing green fluorescence. The most aggregating mutants, WM1–WM5, cause Aβ40 to aggregate more readily than wild-type Aβ42. Amino acid sequences are shown in Fig. 1.

wild-type forms of synthetic peptides (without GFP). Five peptides were synthesized and characterized: WM1 (Gln15→Leu) and WM5 (Asp23→Tyr) were chosen because they are the most aggregating single mutants. These were compared with a peptide corresponding to the clinically isolated Dutch mutant (Glu22→Gln). All of these mutants were synthesized in the context of Aβ40. In addition, two versions of the wild-type sequence, Aβ40 and Aβ42, were also synthesized.

Each peptide was dissolved at 20 μM and incubated at 37 °C under quiescent conditions. At various time points, aliquots were removed and mixed with thioflavin T (ThT), which is widely used to assay for amyloid aggregates.[34] Binding of ThT was quantified by measuring fluorescence at 490 nm. As anticipated from results with the GFP fusions (Fig. 2), mutants WM1 and WM5 have a much higher propensity to aggregate than the corresponding wild-type peptide, Aβ40 (Fig. 3a). Moreover, at early time points (<5 h), WM1 and WM5 aggregate even faster than wild-type Aβ42. This is striking because the mutants were studied in the context of the shorter and less aggregation-prone 40-residue peptide.

After a long incubation (1–2 weeks), Aβ42 produced slightly more aggregation than the WM1 and WM5 mutants in Aβ40 (Fig. 3b). Both Dutch (in the context of Aβ40) and wild-type Aβ40 did not produce significant quantities of amyloid until several days had elapsed. The relatively slow aggregation of the Dutch mutant was unexpected, since it had been reported previously as a mutation that increases aggregation propensity.[35] (Under agitated conditions, the Dutch mutant did indeed aggregate more rapidly than wild-type Aβ40, with ThT fluorescence appearing after 30 min for the Dutch mutant and only after 150 min for wild-type Aβ40; data not shown.)

Mutant peptides rapidly form fibrils

The effects of the mutations on peptide fibrilogenesis were assessed by electron microscopy (EM). Peptides were dissolved at 20 μM in phosphate buffer and incubated under quiescent conditions. EM images were recorded after 1, 3, 7, 14, and 28 days. After 1 day of incubation, fibrils were observed for wild-type Aβ42 and for mutants WM1 and WM5 (Fig. 4a). Again, it is noteworthy that although the WM1 and WM5 mutants were studied in the context of the shorter Aβ40 sequence, they formed fibrils in the same time period as wild-type Aβ42. As shown in Fig. 4a, wild-type Aβ40 and the Dutch mutant of Aβ40 did not show fibrils after 1 day; these peptides formed fibrils more slowly, with fibrils only observed in EM images after a week of incubation (Fig. 4b). The EM results are consistent with the ThT assays: WM1 and WM5 (in the context of Aβ40) and wild-type Aβ42 form fibrils rapidly, whereas the Dutch mutant and wild-type Aβ40 are much slower.

Solubility of mutant peptides

The ThT and EM experiments described above were designed to detect the later steps in Aβ aggregation, namely, the formation of amyloid fibrils. To compare the behavior of mutant and wild-type sequences in the earlier steps of the aggregation pathway, we monitored the disappearance of soluble peptide. Samples at a concentration of 10 μM were incubated at 37 °C under quiescent conditions. After 1 day or 3 days of incubation, the samples were centrifuged at 100,000*g* for 30 min to pellet insoluble material. The amount of soluble peptide remaining in the supernatant was then quantified by reverse-phase (RP) HPLC. In each case, the entire chromatogram was analyzed for the presence of soluble

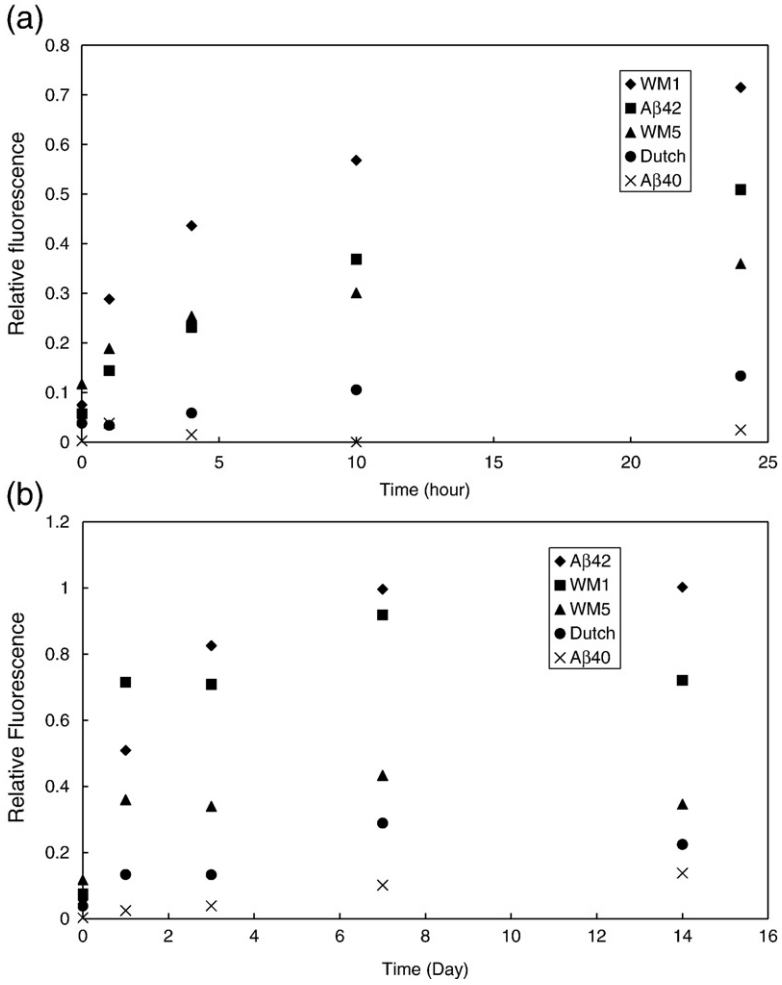

Fig. 3. Time course of ThT fluorescence. Synthetic peptides were incubated for the designated times and then mixed with ThT. All sequences, except for wild-type Aβ42, are in the context of the 40-residue peptide. (a) Relative ThT fluorescence after 0–24 h of incubation. (b) Relative ThT fluorescence after 0–14 days of incubation.

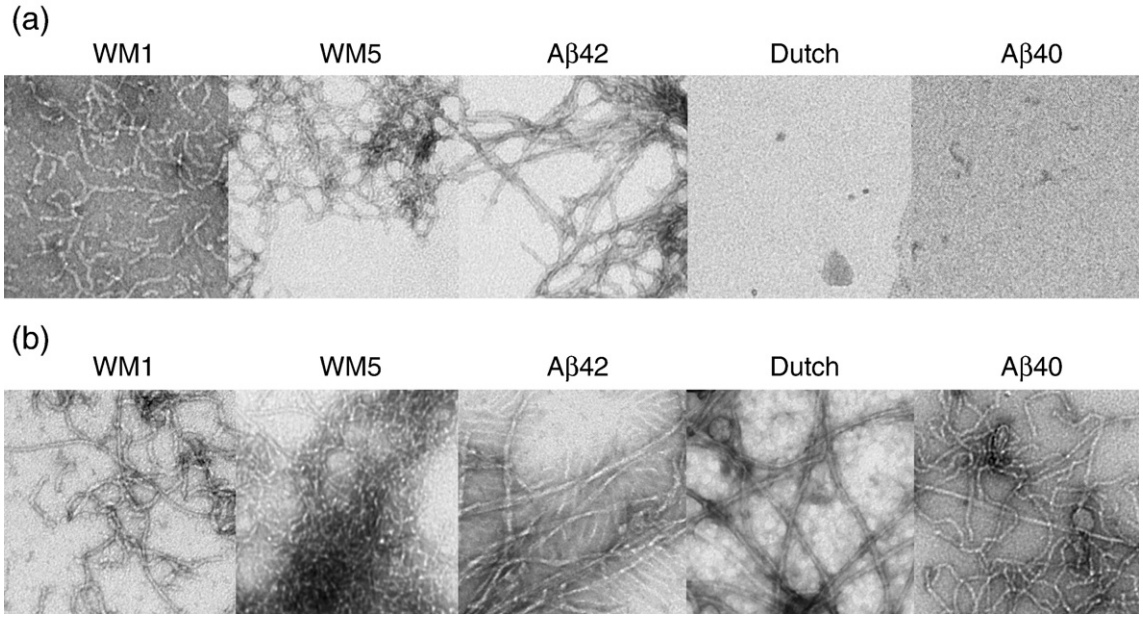

Fig. 4. EM of fibrils imaged after 1 day (a) or 14 days (b) of incubation. All sequences, except for wild-type Aβ42, are in the context of the 40-residue peptide. The WM1 and WM5 mutants form fibrils much faster than either the Dutch or the wild-type version of Aβ40.

peptide corresponding to mutant sequences and/or multimeric species. As shown in Fig. 5, following 1 day of incubation, almost no soluble peptide could be detected for WM5 (Aβ40) or wild-type Aβ42. Thus, these peptides had rapidly aggregated into insoluble material. In contrast, the Dutch mutant and wild-type Aβ40 contained significant soluble peptide even after 3 days of incubation. These results are consistent with the fluorescence data for the GFP fusions (Fig. 2), ThT assays (Fig. 3), and EM analysis (Fig. 4).

The solubility studies of the WM1 mutant produced an unexpected result. WM1 had the lowest fluorescence in the GFP fusion assay and showed the fastest kinetics of fibril formation in the ThT and EM assays, yet a significant amount of WM1 peptide remained soluble after 1 day of incubation. Analysis after 3 days of incubation still revealed soluble peptide (WM1 showed a significant amount of soluble peptide even at 20 μM, the concentration at which ThT and EM assays were performed; data not shown). These observations are discussed below.

Discussion

Amino acid substitutions increase aggregation propensity

We described the construction of an artificial genetic system to screen for amino acid substitutions that increase the aggregation propensity of the Alzheimer's peptide. The screen enabled the isolation and characterization of 20 different mutant sequences of Aβ40. The first 16 of these (WM1–WM16) show unambiguous phenotypes, indicating enhanced aggregation relative to wild-type Aβ40 (Figs. 1 and 2). (WM17–WM20 displayed borderline phenotypes similar to wild type and will not be discussed further.)

Analysis of the 16 sequences with enhanced aggregation propensity (WM1–WM16) shows that *all* of them contain amino acid substitutions that increase hydrophobicity. For example, WM1 has a Gln→Leu mutation, and WM5 has an Asp→Tyr mutation. In another set of examples, WM2 and WM13 both contain a Lys→Thr substitution at the 16th residue. However, WM2 has the additional mutation Ala→Val at position 21, while WM13 has the additional mutation Val→Ala at position 24. Apparently, the increased hydrophobicity of the Ala→Val substitution relative to the Val→Ala substitution accounts for the enhanced aggregation propensity of WM2 relative to WM13 (Fig. 2).

WM5 (Asp23→Tyr), WM9 (Glu22→Ala), and WM17 (Glu22→Asp) have single mutations in the region that forms a turn in structural models of Aβ fibrils.[36–39] This is also true for the clinically isolated mutants, Dutch (Glu22→Gln), Arctic (Glu22→Gly), and Iowa (Asp23→Asn).

As shown in Figs. 1 and 2, WM5 and WM9 lost a charge and showed enhanced aggregation propensity. In contrast, WM17 had a mutation that conserves charge and had an aggregation propensity similar to that of wild-type Aβ40. These data support the hypothesis that increased hydrophobicity and diminished charge enhance aggregation propensity (Chiti *et al.*[29] and see below).

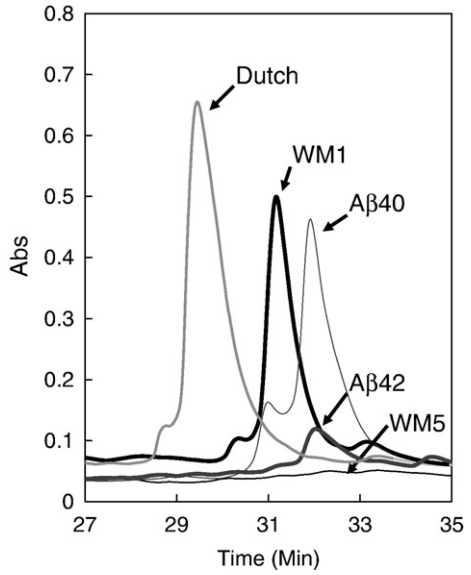

Fig. 5. Peptide solubility. Peptide samples were incubated for 1 day at 37 °C under quiescent conditions. Insoluble material was removed by centrifugation, and supernatants were assayed by RP-HPLC. Wild-type Aβ40 and the Dutch and WM1 mutants of Aβ40 display soluble material. In contrast, the WM5 mutant of Aβ40 and wild-type Aβ42 show minimal quantities of soluble peptide.

Solubility and aggregation

The phenotype of WM1 (Gln15→Leu) in the GFP fusion system showed that this sequence has the highest aggregation propensity of the mutants in the collection (Figs. 1 and 2). The enhanced propensity of WM1 to aggregate was confirmed by biochemical studies with synthetic peptide: Both the ThT assay (Fig. 3) and the EM study (Fig. 4) demonstrate that WM1 forms fibrils much more rapidly than wild-type Aβ40. However, quantification of soluble peptide by HPLC showed that following a full day of incubation, a significant quantity of WM1 peptide remained in solution (Fig. 5). Taken together, these results show that (i) WM1 forms amyloid fibrils rapidly, but (ii), nonetheless, a pool of material remains in solution.

To better understand these results, we analyzed the structural model of Aβ fibrils, built by Petkova *et al.* from solid-state NMR constraints.[36] As shown in Fig. 6, in this model, Gln15 is packed against Val36, Gly37, and Gly38. The mutation of Gln15 to leucine may interfere with this packing and thereby enable a significant fraction of the sample to avoid aggregation and remain in solution. At the same time, the increased hydrophobicity associated with the Gln→Leu substitution might enhance the rate of aggregation for that fraction of the sample that suc-

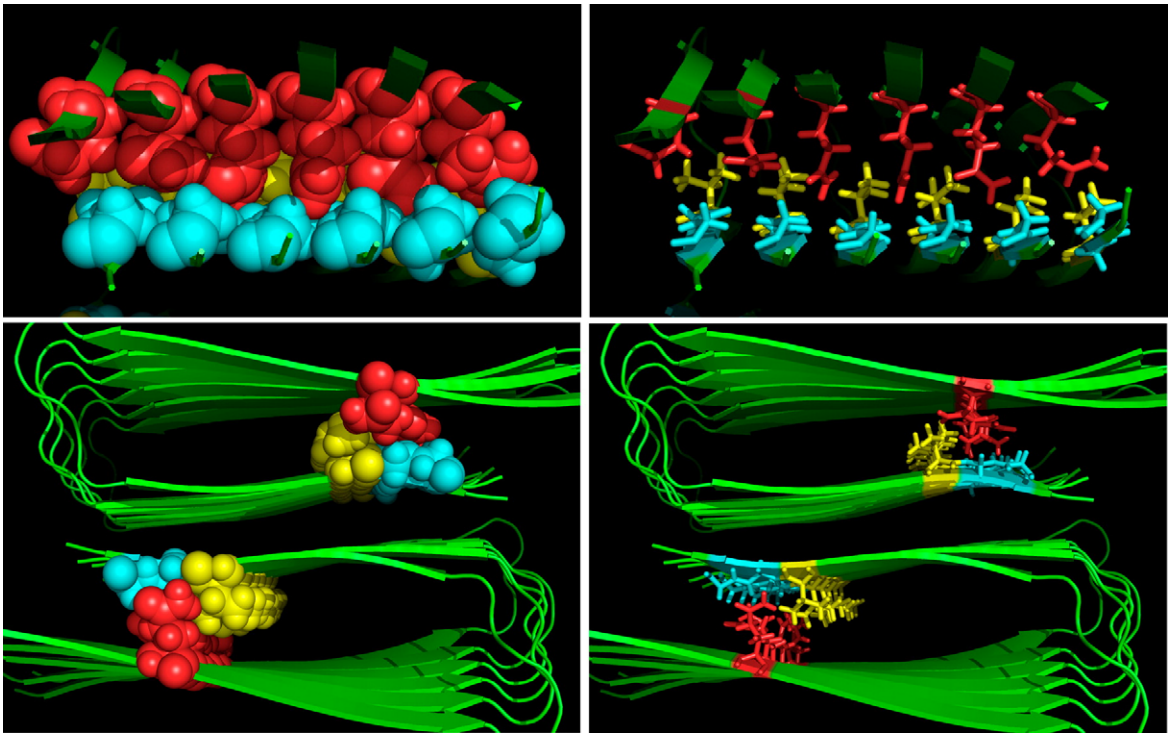

Fig. 6. Model of the structure of Aβ40 fibrils based on solid-state NMR constraints. Gln15 (red) is packed tightly against Val36 (yellow), Gly37 (cyan), and Gly38 (cyan). Coordinates were generously provided by Robert Tycko at the National Institutes of Health. (top) Space-filling (left) and stick (right) models viewed from the side of the fibril. (bottom) Space-filling (left) and stick (right) models viewed along the fibril axis.

cessfully nucleates a structure with altered packing around the Leu side chain. The altered packing around the mutant leucine side chain may account for the observation that the initial fibrils formed by WM1 are shorter than those formed by other peptides (Fig. 4a). A dynamic equilibrium between these short fibrils and monomeric peptide would sustain significant levels of soluble material (Fig. 5).

Comparison with theoretical studies

Which features of an amino acid sequence are responsible for peptide aggregation? Dubay *et al.* formulated a theory to account for aggregation propensity as a function of the following properties: hydrophobicity, β-sheet propensity, α-helix propensity, binary patterning[40] of polar and nonpolar residues, and charge.[41] According to their theory, the aggregation propensity of a sequence (P_{agg}) can be calculated with the following equation:

$$P_{agg} = \alpha_{hyd} I^{hyd} + \alpha_{\alpha} I^{\alpha} + \alpha_{\beta} I^{\beta} + \alpha_{pat} I^{pat} + \alpha_{ch} I^{ch}$$

where I^{hyd}, I^{α},I^{β}, I^{pat}, and I^{ch} are terms corresponding to the hydrophobicity, α-helix propensity, β-sheet propensity, binary patterning, and charge of a sequence, respectively. The coefficients α_{hyd}, α_{α}, α_{β}, α_{pat}, and α_{ch} assign the appropriate weighting for each of these parameters.

The fluorescence of mutant forms of Aβ40 fused to GFP can be compared with the aggregation propensity predicted by this equation. However, it must be noted that aggregation can include the formation of oligomers or fibrils, or both, and recent studies by Luheshi *et al.* indicate that the sequence dependences of the oligomerization and fibrilization rates are similar but not identical.[42] Because we do not know how our mutants affect the relative rates of oligomerization *versus* fibrilization, we have compared the fluorescence of our mutations to the cumulative aggregation rate indicated by the equation above. As shown in Fig. 7, there is a strong inverse correlation between GFP fluorescence (which reports on solubility) and the aggregation propensity predicted by this equation.

Comparison with clinically isolated mutations

The occurrence of early-onset FAD has led to the clinical isolation of several mutations that alter the aggregation behavior of Aβ. Three clinical mutants that have been studied extensively are Dutch (E22Q), Iowa (D23N), and Arctic (E22G). In all three cases, the mutant peptide aggregates into protofibrils and/or fibrils more rapidly than wild-type Aβ.[30,43–45] All three of these mutants contain amino acid substitutions that reduce charge and increase hydrophobicity. However, it is difficult to draw general conclusions about aggregation propensity from a collection comprising only three mutations at two positions in the sequence.

To supplement this naturally occurring collection, we have used an artificial genetic selection to isolate

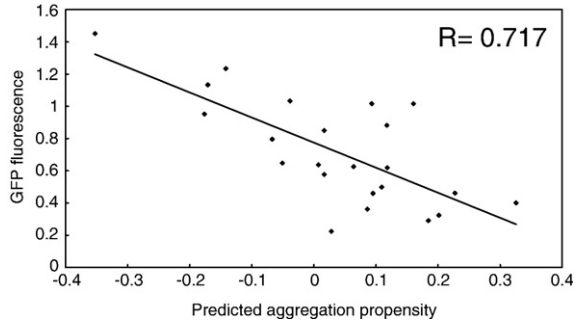

Fig. 7. Correlation between the fluorescence of Aβ40 mutants fused to GFP and the aggregation propensity predicted by the equation of Dubay *et al.*[41] Decreased fluorescence in the GFP system correlates with a prediction for higher aggregation propensity.

novel mutations that enhance Aβ aggregation. This new collection augments the naturally occurring collection in the following ways:

(1) The new collection of mutants is larger and more diverse than the naturally occurring collection. The sequences shown in Fig. 1 comprise 20 mutant sequences with amino acid substitutions at 17 different positions.
(2) Many of the mutations in our collection have dramatic effects on the aggregation propensity of Aβ. Several cause the 40-residue version of Aβ to aggregate more readily than wild-type Aβ42. These mutations have a much greater effect on peptide aggregation than those found in FAD. Indeed, the clinically isolated mutations have subtle effects on peptide aggregation. This is not surprising, since mutations that cause the most dramatic increase in aggregation presumably would be lethal and would not survive in the population. Thus, the studies described here enabled the isolation of mutant substitutions having more dramatic aggregation phenotypes than those found naturally.
(3) The mutations described in this study were isolated using an unbiased screen that does not incorporate any preconceived assumptions about the relationship between amino acid sequence and aggregation propensity. Nonetheless, as illustrated in Figs. 1 and 2, all 16 of our most aggregating mutants contain substitutions that reduce charge and/or increase hydrophobicity. Thus, our studies provide compelling evidence in support of the hypothesis that hydrophobicity is the major determinant of Aβ aggregation.

Materials and Methods

Mutagenesis

Mutagenesis of Aβ40 was performed using nucleotide analogs as described in Zaccolo *et al.*[46] Nucleotide analogs, 2′-deoxy-p-nucleoside-5′-triphosphate, and 8-oxo-2′-deoxyguanosine-5′-triphosphate (Trilink Biotech, San Diego, CA) were used for error-prone PCR using *Taq* polymerase (Promega, Madison, WI). After the first round of PCR, products were purified and used as templates for a second round of PCR to replace the nucleotide analogs with A, G, T, and C. Purified PCR products were double-digested using NdeI and BamHI (NEB, Ipswich, MA) then cloned into a pET28 vector containing the GFP gene.

Screening mutants for enhanced aggregation propensity

Plasmid pET28 vectors containing libraries of mutated Aβ40–GFP fusion genes were transformed into XL1-Blue competent cells (Stratagene, La Jolla, CA) and plated for overnight growth as described previously.[24] Libraries of plasmids from these plates were recovered then transformed into BL21(DE3) (Stratagene) for screening. After transformation, cells were plated onto nitrocellulose filters placed on top of LB plates containing kanamycin (35 μg/ml). After overnight growth at 37 °C, the nitrocellulose filters were transferred onto a plate containing 1 mM IPTG to induce protein expression. To produce the appropriate dynamic range of phenotype, plates were incubated at 30 °C. At this temperature, colonies expressing wild-type Aβ40–GFP fusion appear slightly green.[26] To select mutants with enhanced aggregation propensity, white colonies were picked. Since a white phenotype could also result from the failure of protein expression, all white colonies were also checked for protein expression. Those that expressed at levels similar to the wild-type fusion were sequenced. The GFP fluorescence of each mutant was quantified as described in Ref. 24.

Peptide purification

Crude peptides were purchased from the Keck Institute at Yale University and purified using a C4 RP column. Solvent gradients were run at 65 °C using solvent A (95% water, 5% acetonitrile, and 0.1% trifluoroacetic acid (TFA)) and solvent B (50% acetonitrile, 50% water, and 0.1% TFA). The molecular weights of the purified peptides were confirmed using mass spectrometry, and purity was checked using an analytical RP-HPLC C4 column (Grace Vydac, Deerfield IL). Purified peptides were treated with TFA to remove preexisting aggregates.[47]

ThT assay

Peptides were dissolved in 300 μl dimethyl sulfoxide and diluted with 6 ml of 8 mM NaOH (final peptide concentration, 20 μM). Concentrated phosphate-buffered saline was added to the solution to adjust the pH (final concentration: 50 mM NaH_2PO_4, 100 mM NaCl, and 0.02% NaN_3, pH 7.3–7.4). Samples were incubated at 37 °C under quiescent conditions. At various time points, 500 μl of the sample was mixed with 2.4 ml of ThT solution (7 μM ThT and 50 mM glycerol–NaOH, pH 8.5), and fluorescence was measured at 490 nm (excitation, 450 nm).

Electron microscopy

Solutions were prepared as described above at a peptide concentration of 20 μM. Samples were incubated at 37 °C

under quiescent conditions for 1, 3, 7, 14, 21, and 28 days. Following the incubation, Formvar carbon-coated grids were floated on a drop of each sample for 2 min, washed twice with distilled water, and then stained with 1% uranyl acetate for 2 min. Samples were imaged using a Zeiss 912ab electron microscope.

Detection of soluble peptide

Peptides were dissolved to give a final concentration of 10 μM in 50 mM NaH_2PO_4, 100 mM NaCl, and 0.02% NaN_3 (pH 7.3–7.4). Each sample was incubated at 37 °C under gently agitated or quiescent conditions. After incubation, the samples were centrifuged at 100,000*g* for 30 min to remove insoluble materials, and soluble peptides in the supernatant were quantified by analytical RP-HPLC. Since different mutant peptides and different oligomeric states would be expected to elute at different points in the HPLC gradient, the entire chromatogram was scanned for the presence of peaks corresponding to the elution of any soluble species of peptide.

Acknowledgement

We thank Margaret Bisher for assistance with the electron microscopy.

References

1. Selkoe, D. J. (2001). Alzheimer's disease: genes, proteins, and therapy. *Physiol. Rev.* **81**, 741–766.
2. Roher, A. E., Lowenson, J. D., Clarke, S., Woods, A. S., Cotter, R. J., Gowing, E. & Ball, M. J. (1993). β-Amyloid-(1–42) is a major component of cerebrovascular amyloid deposits: implications for the pathology of Alzheimer disease. *Proc. Natl Acad. Sci. USA*, **90**, 10836–10840.
3. Jarrett, J. T., Berger, E. P. & Lansbury, P. T., Jr (1993). The carboxy terminus of the β-amyloid protein is critical for the seeding of amyloid formation: implications for the pathogenesis of Alzheimer's disease. *Biochemistry*, **32**, 4693–4697.
4. Harper, J. D. & Lansbury, P. T., Jr (1997). Models of amyloid seeding in Alzheimer's disease and scrapie: mechanistic truths and physiological consequences of the time-dependent solubility of amyloid proteins. *Annu. Rev. Biochem.* **66**, 385–407.
5. Hardy, J. A. & Higgins, G. A. (1992). Alzheimer's disease: the amyloid cascade hypothesis. *Science*, **256**, 184–185.
6. Tomita, T., Tokuhiro, S., Hashimoto, T., Aiba, K., Saido, T. C., Maruyama, K. & Iwatsubo, T. (1998). Molecular dissection of domains in mutant presenilin 2 that mediate overproduction of amyloidogenic forms of amyloid β-peptides. *J. Biol. Chem.* **273**, 21153–21160.
7. Ikeuchi, T., Dolios, G., Kim, S.-H., Wang, R. & Sisodia, S. S. (2003). Familial Alzheimer disease-linked presenilin 1 variants enhanced production of both Aβ1–40 and Aβ1–42 peptides that are only partially sensitive to a potent aspartyl protease transition state inhibitor of "γ-secretase". *J. Biol. Chem.* **278**, 7010–7018.
8. De Jonghe, C., Zehr, C., Yager, D., Prada, C.-M., Younkin, S., Hendriks, L. *et al.* (1998). Flemish and Dutch mutations in amyloid β precursor protein have different effects on amyloid β secretion. *Neurobiol. Dis.* **5**, 281–286.
9. Sun, X., Tong, Y., Qing, H., Chen, C.-H. & Song, W. (2006). Increased BACE1 maturation contributes to the pathogenesis of Alzheimer's disease in Down syndrome. *FASEB J.* **20**, 1361–1368.
10. Cataldo, A. M., Petanceska, S., Terio, N. B., Peterhoff, C. M., Durham, R., Mercken, M. *et al.* (2004). Aβ localization in abnormal endosomes: association with earliest Aβ elevations in AD and Down syndrome. *Neurobiol. Aging*, **25**, 1263–1272.
11. Head, E. & Lott, I. T. (2004). Down syndrome and β-amyloid deposition. *Curr. Opin. Neurol.* **17**, 95–100.
12. Teller, J. K., Russo, C., DeBusk, L. M., Angelini, G., Zaccheo, D., Dagna-Bricarelli, F. *et al.* (1996). Presence of soluble amyloid β-peptide precedes amyloid plaque formation in Down's syndrome. *Nat. Med.* **2**, 93–95.
13. Johnson-Wood, K., Lee, M., Motter, R., Hu, K., Gordon, G., Barbour, R. *et al.* (1997). Amyloid precursor protein processing and Aβ42 deposition in a transgenic mouse model of Alzheimer disease. *Proc. Natl Acad. Sci. USA*, **94**, 1550–1555.
14. Crowther, D. C., Kinghorn, K. J., Miranda, E., Page, R., Curry, J. A., Duthie, F. A. *et al.* (2005). Intraneural Aβ, non-amyloid aggregates and neurodegeneration in a *Drosophila* model of Alzheimer's disease. *Neuroscience*, **132**, 123–135.
15. Link, C., Taft, A., Kapulkin, V., Duke, K., Kim, S., Fei, Q. *et al.* (2003). Gene expression analysis in a transgenic *Caenorhabditis elegans* Alzheimer's disease model. *Neurobiol. Aging*, **24**, 397–413.
16. Wang, D.-S., Dickson, D. W. & Malter, J. S. (2006). β-Amyloid degradation and Alzheimer's disease. *J. Biomed. Biotechnol.* **2006**, 1–12.
17. Miners, J. S., Van Helmond, Z., Chalmers, K., Wilcock, G., Love, S. & Kehoe, P. G. (2006). Decreased expression and activity of neprilysin in Alzheimer disease are associated with cerebral amyloid angiopathy. *J. Neuropathol. Exp. Neurol.* **65**, 1012–1021.
18. Eckman, E. A., Adams, S. K., Troendle, F. J., Stodola, B. A., Kahn, M. A., Fauq, A. H. *et al.* (2006). Regulation of steady-state β-amyloid levels in the brain by neprilysin and endothelin-converting enzyme but not angiotensin-converting enzyme. *J. Biol. Chem.* **281**, 30471–30478.
19. Russo, R., Borghi, R., Markesbery, W., Tabaton, M. & Piccini, A. (2005). Neprilysin decreases uniformly in Alzheimer's disease and in normal aging. *FEBS Lett.* **579**, 6027–6030.
20. Poirier, R., Wolfer, D. P., Welzl, H., Tracy, J., Galsworthy, M. J., Nitsch, R. M. & Mohajeri, M. H. (2006). Neuronal neprilysin overexpression is associated with attenuation of Aβ-related memory deficit. *Neurobiol. Dis.* **24**, 475–483.
21. Lesne, S., Koh, M. T., Kotilinek, L., Kayed, R., Glabe, C. G., Yang, A. *et al.* (2006). A specific amyloid-β protein assembly in the brain impairs memory. *Nature*, **440**, 352–357.
22. Walsh, D. M., Townsend, M., Podlisny, M. B., Shankar, G. M., Fadeeva, J. V., Agnaf, O. E. *et al.* (2005). Certain inhibitors of synthetic amyloid β-peptide (Aβ) fibrillogenesis block oligomerization of natural Aβ and thereby rescue long-term potentiation. *J. Neurosci.* **25**, 2455–2462.
23. Walsh, D. M., Klyubin, I., Fadeeva, J. V., Cullen, W. K., Anwyl, R., Wolfe, M. S. *et al.* (2002). Naturally secreted

oligomers of amyloid-β protein potently inhibit hippocampal long-term potentiation *in vivo*. *Nature*, **416**, 535–539.
24. Wurth, C., Guimard, N. K. & Hecht, M. H. (2002). Mutations that reduce aggregation of the Alzheimer's Aβ42 peptide: an unbiased search for the sequence determinants of Aβ amyloidogenesis. *J. Mol. Biol.* **319**, 1279–1290.
25. Kim, W. & Hecht, M. H. (2006). Generic hydrophobic residues are sufficient to promote aggregation of the Alzheimer's Aβ42 peptide. *Proc. Natl Acad. Sci. USA*, **103**, 15824–15829.
26. Kim, W. & Hecht, M. H. (2005). Sequence determinants of enhanced amyloidogenicity of Alzheimer Aβ42 peptide relative to Aβ40. *J. Biol. Chem.* **280**, 35069–35076.
27. Williams, A. D., Portelius, E., Kheterpal, I., Guo, J., Cook, K. D., Xu, Y. & Wetzel, R. (2004). Mapping Aβ amyloid fibril secondary structure using scanning proline mutagenesis. *J. Mol. Biol.* **335**, 833–842.
28. Morimoto, A., Irie, K., Murakami, K., Masuda, Y., Ohigashi, H., Nagao, M. *et al.* (2004). Analysis of the secondary structure of β-amyloid (Aβ42) fibrils by systematic proline replacement. *J. Biol. Chem.* **27**, 52781–52788.
29. Chiti, F., Stefani, M., Taddei, N., Ramponi, G. & Dobson, C. M. (2003). Rationalization of the effects of mutations on peptide and protein aggregation rates. *Nature*, **424**, 805–808.
30. Massi, F., Klimov, D., Thirumalai, D. & Straub, J. E. (2002). Charge states rather than propensity for β-structure determine enhanced fibrillogenesis in wild-type Alzheimer's β-amyloid peptide compared to E22Q Dutch mutant. *Protein Sci.* **11**, 1639–1647.
31. Waldo, G. S., Standish, B. M., Berendzen, J. & Terwilliger, T. C. (1999). Rapid protein-folding assay using green fluorescent protein. *Nat. Biotechnol.* **17**, 691–695.
32. Kim, W., Kim, Y., Min, J., Kim, D., Chang, Y. & Hecht, M. (2006). A high-throughput screen for compounds that inhibit aggregation of the Alzheimer's peptide. *ACS Chem. Biol.* **1**, 461–469.
33. Jarrett, J. T. & Lansbury, P. T., Jr (1993). Seeding "one-dimensional crystallization" of amyloid: a pathogenic mechanism in Alzheimer's disease and scrapie? *Cell*, **73**, 1055–1058.
34. Levine, H., III (1993). Thioflavin T interaction with synthetic Alzheimer's disease β-amyloid peptides: detection of amyloid aggregation in solution. *Protein Sci.* **2**, 404–410.
35. Davis, J. & Van Nostrand, W. E. (1996). Enhanced pathologic properties of Dutch-type mutant amyloid β-protein. *Proc. Natl Acad. Sci. USA*, **93**, 2996–3000.
36. Petkova, A. T., Yau, W.-M. & Tycko, R. (2006). Experimental constraints on quaternary structure in Alzheimer's β-amyloid fibrils. *Biochemistry*, **45**, 498–512.
37. Petkova, A. T., Leapman, R., Guo, Z., Yau, W., Mattson, M. & Tycko, R. (2005). Self-propagating, molecular-level polymorphism in Alzheimer's β-amyloid fibrils. *Science*, **307**, 262–265.
38. Petkova, A., Ishii, Y., Balbach, J., Antzutkin, O., Leapman, R., Delaglio, F. & Tycko, R. (2002). A structural model for Alzheimer's β-amyloid fibrils based on experimental constraints from solid state NMR. *Proc. Natl Acad. Sci. USA*, **99**, 16742–16747.
39. Lührs, T., Ritter, C., Adrian, M., Riek-Loher, D., Bohrmann, B., Döbeli, H. *et al.* (2005). 3D structure of Alzheimer's amyloid-β(1–42) fibrils. *Proc. Natl Acad. Sci. USA*, **102**, 17342–17347.
40. Broome, B. M. & Hecht, M. H. (2000). Nature disfavors sequences of alternating polar and nonpolar amino acids: implications for amyloidogenesis. *J. Mol. Biol.* **296**, 961–968.
41. Dubay, K. F., Pawar, A. P., Chiti, F., Zurdo, J., Dobson, C. M. & Vendruscolo, M. (2004). Prediction of the absolute aggregation rates of amyloidogenic polypeptide chains. *J. Mol. Biol.* **341**, 1317–1326.
42. Luheshi, L. M., Tartaglia, G. G., Brorsson, A. C., Pawar, A. P., Watson, I. E., Chiti, F. *et al.* (2007). Systematic *in vivo* analysis of the intrinsic determinants of amyloid β pathogenicity. *PLoS Biol.* **5**, 2493–2500.
43. Van Nostr, W. E., Melchor, J. P., Cho, H. S., Greenberg, S. M. & Rebeck, G. W. (2001). Pathogenic effects of D23N Iowa mutant amyloid β-protein. *J. Biol. Chem.* **276**, 32860–32866.
44. Nilsberth, C., Westlind-Danielsson, A., Eckman, C. B., Condron, M. M., Axelman, K., Forsell, C. *et al.* (2001). The 'Arctic' APP mutation (E693G) causes Alzheimer's disease by enhanced Aβ protofibril formation. *Nat. Neurosci.* **4**, 887–893.
45. Whalen, B., Selkoe, D. J. & Hartley, D. (2005). Small non-fibrillar assemblies of amyloid-β protein bearing the Arctic mutation induce rapid neuritic degeneration. *Neurobiol. Dis.* **20**, 254–266.
46. Zaccolo, M., Williams, D., Brown, D. & Gherardi, E. (1996). An approach to random mutagenesis of DNA using mixtures of triphosphate derivatives of nucleoside analogues. *J. Mol. Biol.* **255**, 589–603.
47. Jao, S., Ma, K., Talafous, J., Orlando, R. & Zagorski, M. G. (1997). Trifluoroacetic acid pretreatment reproducibly disaggregates the amyloid-β peptide. *Amyloid J. Int. Exp. Clin. Invest.* **4**, 240–252.